Monthly Notices of the ROYAL ASTRONOMICAL SOCIETY

MNRAS **533,** 4268–4273 (2024) https://doi.org/10.1093/mnras/stae1880
Advance Access publication 2024 August 05

Searching for pulsars, magnetars, and fast radio bursts in the sculptor galaxy using MeerKAT

H. Hurter [1]★ C. Venter [1,2] L. Levin,[3] B. W. Stappers [3] E. D. Barr [4] R. P. Breton [3] S. Buchner,[5] E. Carli [3] M. Kramer [4] P. V. Padmanabh,[6,7,4] A. Possenti,[8] V. Prayag[9,10] and J. D. Turner [3]

[1]*Centre for Space Research, North-West University, Private Bag X6001, Potchefstroom 2520, South Africa*
[2]*National Institute for Theoretical and Computational Sciences (NITheCS), Stellenbosch, South Africa.*
[3]*Jodrell Bank Centre for Astrophysics, Department of Physics and Astronomy, The University of Manchester, M13 9PL Manchester, UK*
[4]*Max-Planck-Institut für Radioastronomie, Auf dem Hügel 69, D-53121 Bonn, Germany*
[5]*South African Radio Astronomy Observatory (SARAO), 2 Fir Street, Black River Park, Observatory, 7925 Cape Town, South Africa*
[6]*Max Planck Institute for Gravitational Physics (Albert Einstein Institute), D-30167 Hannover, Germany*
[7]*Leibniz Universität Hannover, D-30167 Hannover, Germany*
[8]*INAF-Osservatorio Astronomico di Cagliari, via della Scienza 5, Ī-09047 Selargius (CA), Italy*
[9]*Department of Astronomy, The University of Cape Town, Private Bag X3, Rondebosch 7701, Cape Town, South Africa*
[10]*High Energy Physics, Cosmology & Astrophysics Theory (HEPCAT) Group, Department of Mathematics & Applied Mathematics, University of Cape Town, 7700 Cape Town, South Africa*

Accepted 2024 July 30. Received 2024 July 26; in original form 2024 June 7

ABSTRACT

The Sculptor Galaxy (NGC 253), located in the Southern Hemisphere, far off the Galactic Plane, has a relatively high star-formation rate of about 7 $M_\odot\,yr^{-1}$ and hosts a young and bright stellar population, including several super star clusters and supernova remnants. It is also the first galaxy, apart from the Milky Way Galaxy to be associated with two giant magnetar flares. As such, it is a potential host of pulsars and/or fast radio bursts in the nearby Universe. The instantaneous sensitivity and multibeam sky coverage offered by MeerKAT therefore make it a favourable target. We searched for pulsars, radio-emitting magnetars, and fast radio bursts in NGC 253 as part of the TRAPUM large survey project with MeerKAT. We did not find any pulsars during a 4 h observation, and derive a flux density limit of 4.4 μJy at 1400 MHz, limiting the pseudo-luminosity of the brightest putative pulsar in this galaxy to 54 Jy kpc^2. Assuming universality of pulsar populations between galaxies, we estimate that detecting a pulsar as bright as this limit requires NGC 253 to contain a pulsar population of $\gtrsim$20 000. We also did not detect any single pulses, and our single pulse search flux density limit is 62 mJy at 1284 MHz. Our search is sensitive enough to have detected any fast radio bursts and radio emission similar to the brighter pulses seen from the magnetar SGR J1935+2154 if they had occurred during our observation.

Key words: stars: neutron – pulsars: general – Galaxy: general – galaxies: individual: NGC 253 – radio continuum: transients.

1 INTRODUCTION

The detection and monitoring of radio pulsars, given their powerful magnetic fields, extreme compactness, and broad-band electromagnetic radiation, are important in a variety of disciplines, such as exploring General Relativistic effects (Taylor, Fowler & McCulloch 1979), the equation of state of neutron stars (NSs; e.g. Koehn et al. 2024), as well as relativistic plasma and radiation physics (e.g. Philippov & Kramer 2022). Currently, the Milky Way (MW) galaxy hosts more than 99 per cent (3608 to date) of the known radio pulsar population (Manchester et al. 2005).[1] The remaining 41 pulsars are extragalactic and were discovered in two satellite galaxies of the MW, the Magellanic clouds (e.g. Crawford et al. 2001; Manchester et al. 2006; Titus et al. 2019; Hisano et al. 2022; Carli et al. 2024). The Magellanic clouds are considered to be good targets for pulsar searches, since they are not obstructed by the Galactic plane, and therefore searches are not greatly affected by dispersive effects of the Galactic interstellar medium. Furthermore, the Magellanic Clouds host diverse NS populations that are indicative of various evolutionary stages of massive stars, and a large number of supernova remnants (see e.g. Badenes, Maoz & Draine 2010; Titus et al. 2020), which further motivates the pulsar searches in these types of environment. NSs are created by core-collapse events of stars with masses between 8–25 $M_\odot$ depending on their metallicity and binary companion (Heger et al. 2003). Considering factors such as star formation history, stellar mass distributions, and stellar types of galaxy targets is important for pulsar searches. For instance, recent star-forming episodes produce populations of NSs that may be detectable as radio pulsars.

★ E-mail: heinrich.hurter11@gmail.com
[1]ATNF catalogue version 2.3.0: https://www.atnf.csiro.au/research/pulsar/psrcat/.

An increasing number of fast radio bursts (FRBs) have been detected in the last few decades. FRBs are classified by their one-off or multiple short-duration bursts (Lorimer et al. 2007; Thornton et al. 2013; Spitler et al. 2016), and it is accepted that FRBs are extragalactic events due to the high associated dispersion measure (DM) that puts them well beyond the MW limits (e.g. Platts et al. 2019). The mechanisms responsible for repeating and non-repeating bursts are still a matter of debate. With the detection and localization of more bursts, constraints can be placed on their emission mechanism (e.g. CHIME/FRB Collaboration et al. 2021). A possible explanation for non-repeating FRBs is that they are an after-effect of cataclysmic events (e.g. Marnoch et al. 2020). On the contrary, repeating FRBs should have a non-cataclysmic origin (Spitler et al. 2016). A recent detection of FRB-like bursts was made from the Soft-Gamma Repeater (SGR) J1935+2154, which is a Galactic magnetar. This suggests a strong connection between magnetar emission and at least some repeating FRBs (Camilo et al. 2006; Bochenek et al. 2020; CHIME/FRB Collaboration et al. 2020). Furthermore, SGRs are associated with regions of recent star-forming and supernovae (Gaensler 2004). Known FRB host galaxies exhibit a wide range of compositions, with masses in the range $M_* = 10^8$–$10^{10}\,\mathrm{M}_\odot$ and star-formation rates (SFRs) ranging from 0.05–10 $\mathrm{M}_\odot\,\mathrm{yr}^{-1}$ (Bhandari et al. 2022). Mannings et al. (2021) found that all FRBs located in hosts with spiral structures occur near or on a spiral arm.

The Nearby Galaxies programme within the TRansients And PUlsars with MeerKAT (TRAPUM[2]). Large Survey Project (Stappers & Kramer 2016) has as one of its aims the discovery of new pulsars and fast transients outside of the MW galaxy, and to investigate their properties in relation to those of their host galaxy. One of the targets of this survey is NGC 253, also known as the Sculptor Galaxy. It is located in the southern sky far below the Galactic Plane, at a Galactic latitude of $b = -87.96^\circ$ and a distance of 3.5 ± 0.2 Mpc (Rekola et al. 2005). It is a promising target for finding pulsars due to its population of massive stars and its similarity to the MW. It is classified as a barred spiral galaxy and is one of the nearest galaxies undergoing a nuclear starburst. It is one of the brightest starburst galaxies in the Southern Hemisphere, with detections of numerous supernova remnants (SNRs) within the starburst region, including one optically identified supernova (SNR 1940E, Zwicky 1941; Chhetri et al. 2018) close to the central region of the galaxy. The unobscured stellar population is consistent with ages < 8 Myr (Kornei & McCrady 2009; Davidge 2016). The centre hosts a population of more than a dozen super star clusters (SSC) that are still in the formative stages. A near-infrared photometry study of this galaxy revealed 181 star clusters in the central 600 pc (Camperi et al. 2022). Nine of these clusters have masses in the range of 10^5–$10^6\,\mathrm{M}_\odot$ and ages less than 7 Myr, with the remaining clusters being older and less massive. This is interesting since these clusters can provide insights into the star formation history of this galaxy. NGC 253 has a total mass of $(8.1 \pm 2.6) \times 10^{11}\,\mathrm{M}_\odot$ (Karachentsev et al. 2021), which is about a factor of two less than the total mass of the MW. Forbes et al. (1993) suggested that the central 6 arcsec of NGC 253 contains about 24 000 O-type stars and that SNRs are located throughout the nuclear region. The nucleus has an SFR of approximately $5\,\mathrm{M}_\odot\,\mathrm{yr}^{-1}$, which accounts for about 70 per cent of the rate of the entire galaxy (Wik et al. 2014). The central SFR of NGC 253 is 30–40 times higher than that of the central region of the MW (Longmore et al. 2013; Barnes et al. 2017; Mills et al. 2021). A high SFR is consistent with a young stellar population (Duarte Puertas et al. 2022), which in turn is likely to contribute to a large SNR population. Furthermore, Wik et al. (2014) found that X-ray emission above $\gtrsim$10 keV were concentrated in the central 100 arcsec of NGC 253, produced by three nuclear sources, an off-nuclear ultraluminous X-ray source and a pulsar candidate, which could be an extremely luminous X-ray pulsar. NGC 253 is furthermore the first galaxy to be associated with two magnetar giant flares (MGFs), (Gamma-Ray Burst) GRB 180128A and GRB 200415A (Svinkin et al. 2021; Trigg et al. 2024). GRB 200415A was observed on 2020 April 15, located in an area of 20 arcmin^2 that overlaps the central region of NGC 253 (Svinkin et al. 2021). GRB 180128A occured 808 days before GRB 200415A on 2018 January 28, and was found in archival data after the discovery of GRB 200415A. However, it is still unclear whether these bursts originated from the same magnetar (Trigg et al. 2024). The formation channel of magnetars is consistent with core-collapse supernovae (Heintz et al. 2020; Bochenek, Ravi & Dong 2021). Thus, the high SFR, the presence of SNRs, the high energy X-ray sources, young star clusters, and associated MGFs support the likelihood that NGC 253 contains a young NS/pulsar population. It is also interesting to note that young pulsars sometimes emit giant radio pulses (Lundgren et al. 1995; Geyer et al. 2021), which would enable us to discover distant radio pulsars that might otherwise not be detectable (McLaughlin & Cordes 2003). The probable presence of at least one magnetar in this galaxy also means that there may be sources responsible for emitting FRB-like pulses, like those seen from SGR J1935−2154.

Extragalactic targets such as NGC 253, NGC 300, NGC 6300, NGC 7793, and Fornax were previously searched for giant radio pulses using a single beam from the Parkes (Murriyang) Telescope, but none were detected (McLaughlin & Cordes 2003). Two pulsar search surveys (see Section 4) also conducted short integration pulsar searches in the direction of NGC 253. However, these searches did not yield evidence for pulsars in NGC 253.

We made use of the exceptional sensitivity of the MeerKAT Radio Telescope to perform a new deeper pulsar and FRB search. The MeerKAT Radio Telescope is a radio interferometer located in the Northern Cape region of South Africa and has remarkable sensitivity for pulsar and fast transient searches. MeerKAT is made up of 64 parabolic antennas, each with a diameter of 13.5 m, distributed to form a maximum baseline of 8 km (Jonas & MeerKAT Team 2016; Camilo 2018). The gain of the fully phased array is about 4 times higher than that of the Parkes Telescope and 1.4 times higher than that of the Green Bank Telescope (Bailes et al. 2020), therefore making the MeerKAT Radio Telescope even more suitable for extragalactic transient searches.

In this article, we describe our observation of NGC 253 and data reduction methods in Section 2. We present our results and search sensitivities in Section 3. Our conclusions follow in Section 4.

2 TRAPUM OBSERVATION

We observed NGC 253 on 2022 October 5 for a total integration time of 14 085.3 s. The observation used 44 MeerKAT antennas within the approximately 1 km baseline to create coherent beams that were big enough to cover the entire galaxy, and was carried out at *L*-band, with a central frequency of $f_c = 1.284$ GHz, and a bandwidth of $\Delta f = 856$ MHz. The frequency band was divided into 2048 frequency channels and data were sampled every 153 µs. Beamforming was performed using the Filterbanking BeamFormer User-Supplied Equipment (FBFUSE; Barr 2017), which created 768 synthesized elliptically-shaped coherent beams for the observation. The shape and orientation of the coherent beams are dependent on

[2]https://www.trapum.org

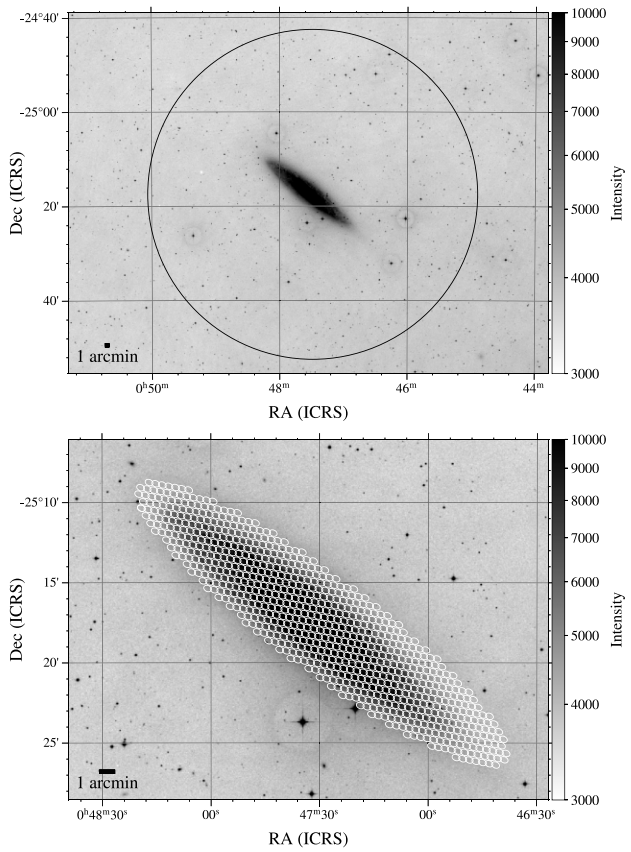

Figure 1. An image of NGC 253 from the Digitised Sky Survey (DSS2) in the near-infrared (NIR) band. The incoherent beam can be seen in the upper plot, and was centered on SN 1940E. Positions of the 768 elliptical coherent beams overlaid on NGC 253 shown in the lower panel.

the position of the target (Chen et al. 2021). We used MOSAIC[3] (Chen et al. 2021), a PYTHON package that simulates one coherent beam with the observational parameters and tiles a specified number of beams at various positions and overlaps them appropriately at a chosen sensitivity level. The tiling pattern is illustrated in the lower panel of Fig. 1. The neighbouring beams overlapped at 75 per cent of their peak sensitivity, which ensures that coherent sensitivity is not degraded by more than this amount across the searched area. Data processing was performed on the Accelerated Pulsar Search User-Supplied Equipment (APSUSE; Barr 2017), which is a dedicated pulsar processing computer cluster. We performed a periodicity search with PEASOUP[4] (Barr 2020, described in Morello et al. 2018), which is a GPU-based pulsar search algorithm that implements various processing steps such as dedispersion, low-frequency noise removal, and applying a Fast Fourier Transform (FFT). The mitigation of radio frequency interference (RFI) was performed with PULSARX's[5] `filtool` (Men et al. 2023). We generated a dedispersion plan with PRESTO's[6] `DDplan.py` script (Ransom 2011), which was then used to efficiently dedisperse the data based on the observational parameters. PEASOUP uses the DEDISP[7] package (part of the PEASOUP suite; Barsdell et al. 2012; Levin 2012) to perform dedispersion up to a value of 500 pc cm^{-3}. The expected DM along the line of sight for NGC 253 is approximately 19 and 29 pc cm^{-3} based on the YMW16 and NE2001 electron density models, respectively (Cordes & Lazio 2003; Yao, Manchester & Wang 2017). An acceleration search for pulsars in binaries up to $\pm 20\,\mathrm{ms}^{-2}$, assuming constant acceleration, was performed. These parameters were chosen in view of computing constraints. An acceleration tolerance of 10 per cent was chosen, implying that the acceleration broadening from one acceleration step to the next cannot exceed 10 per cent of the combined pulse smearing (Levin 2012). Furthermore, the candidates were harmonically summed by PEASOUP to the fourth harmonic. We also applied default channel and period masks representative of RFI sources that are known to corrupt the MeerKAT *L*-band. Candidates were then clustered together by PEASOUP and candidates with periodicities corresponding to known interference were removed. This was followed by a two-stage multibeam candidate filtering performed by CANDIDATE_FILTER[8], with a candidate spectral signal-to-noise (S/N) threshold of 9.5. Furthermore, candidates with similar periodicities were clustered together, and a spatial domain multibeam coincidencing algorithm was applied. This algorithm is used to characterize potential pulsar detections between adjacent beams and distinguish them from RFI sources that are spread over numerous neighbouring beams (see Padmanabh et al. 2023). The remaining candidates were folded at the parameters (DM, spin period, acceleration) obtained from PEASOUP, using `psrfold_fil` from PULSARX (Men et al. 2023) and scored with PICS, a Pulsar Image-based Classification System based on machine learning that was trained on data from the PALFA survey (Zhu et al. 2014). PICS generates a number between 0 and 1 for each candidate, with 1 representing potential pulsar detection and 0 RFI or noise. We cut the candidates up to a minimum score of 0.1. This left us with 2415 pulsar candidates viewed with CANDYJAR[9]. The S/N distribution of these candidates is consistent with the tail of a noise distribution, with candidates outside of this range identified as RFI. Padmanabh et al. (2023) contains additional details on the TRAPUM search pipeline. Furthermore, we also conducted a single pulse search using TRANSIENTX[10], which is a high-performance single pulse search software (Men & Barr 2024). TRANSIENTX is designed to search successive data blocks, typically a few seconds in duration. Each data block undergoes various processing stages, such as mitigating RFI, dedispersion, matched filtering, clustering, and plotting (see Men & Barr 2024 for details on the algorithm). We searched for pulses with a width up to 0.1 s over a DM range 0–5000 pc cm^{-3} to accommodate high DMs at which these transients can be detected. A S/N threshold of 8.0 was applied and candidates above this threshold were retained for viewing. We further reduced the number of candidates by removing four short time segments containing RFI. This left us with 2314 candidates, and the diagnostic plots (showing the single pulse summed over all frequencies, a grey-scale of the intensity of the pulse as a function of frequency, and a grey-scale of the S/N of the pulse versus DM and time) generated by TRANSIENTX were viewed manually. All candidates viewed were consistent with noise or RFI.

[3] https://gitlab.mpifr-bonn.mpg.de/wchen/Beamforming/tree/master/mosaic
[4] https://github.com/ewanbarr/peasoup
[5] https://github.com/ypmen/PulsarX
[6] https://github.com/scottransom/presto
[7] https://github.com/ewanbarr/dedisp
[8] https://github.com/prajwalvp/candidate_filter
[9] https://github.com/vivekvenkris/CandyJar
[10] https://github.com/ypmen/TransientX

3 SEARCH SENSITIVITY AND UPPER LIMITS

Our pulsar search returned no significant candidates during the 4 h observation. We therefore derived a flux density limit for our pulsar search using a modified radiometer equation from (Dewey et al. 1985):

$$S_{\rm lim} = \beta \frac{(S/N)T_{\rm sys}}{\epsilon G \sqrt{n_{\rm p} t_{\rm int} \Delta f}} \sqrt{\frac{D}{1-D}}, \quad (1)$$

where S/N is the spectral S/N threshold of 9.5, β is the correction factor due to digitization. Since the loss of telescope sensitivity due to 8-bit digitization is minimal, we have $\beta = 1$ (Kouwenhoven & Voûte 2001). A conversion efficiency factor $\epsilon = 0.7$ for converting from spectral S/N to folded S/N (Morello et al. 2020). The system temperature is the sum of the receiver temperature ($T_{\rm rec} = 18$ K, Bailes et al. 2020) and the sky temperature contribution $T_{\rm sky} \approx 4.24$ K (Zheng et al. 2017)[11] in the direction of NGC 253. The telescope gain is $G = 1.925\,{\rm K\,Jy^{-1}}$ for the core array in coherent mode ($G = 0.34\,{\rm KJy^{-1}}$ for incoherent mode with 61 antennas). Lastly, the number of polarizations is $n_{\rm p} = 2$, the bandwidth $\Delta f = 856$ MHz, and the integration time $t_{\rm int} = 14\,085.30$ s. We assume a pulsar duty cycle of $D = 2.5$ per cent, which is the median intrinsic pulsar duty cycle excluding millisecond pulsars and pulsars in globular clusters, rotating radio transients, magnetars, and binary pulsars, taken from the ATNF catalogue (Manchester et al. 2005), and a spectral index of -1.6 (Jankowski et al. 2018). Thus, the minimum detectable flux density for our periodicity search is $S_{\rm lim,1400MHz} = 4.4$ μJy at the centre of the incoherent beam and of a coherent beam for a pulsar with a period of 100 ms and above at a DM = 250 pc cm^{-3}. At lower spin periods, factors such as dispersion smearing, sampling time, and scattering influence the detectability of such short-period pulsars. The corresponding pseudo-luminosity limit, which is calculated using

$$L_{1400} = S_{1400} d^2, \quad (2)$$

is about 54 Jy kpc^2 for a distance of $d = 3.5$ Mpc.

For our fast transient search, none of the remaining candidates yielded any promising detections for FRBs or FRB-like pulses. Therefore, we also derived the sensitivity limit of our transient search by using the radiometer equation

$$S_{\rm pulse\,peak} = \frac{(S/N)S_{\rm sys}}{\sqrt{n_{\rm p} \Delta f W}}, \quad (3)$$

(e.g. McLaughlin & Cordes 2003). Here, W is the observed width of the pulse. We assume an intrinsic pulse width of 1 ms at a DM of 500 pc cm^{-3}. We also take into consideration the dispersive smearing across individual channels and the smearing due to sampling time. $S_{\rm sys}$ is the equivalent system flux density ($T_{\rm sys}/G$). We calculated a single pulse flux density limit of $S_{\rm peak,1284GHz} \simeq 62$ mJy. Fig. 2 shows which astronomical objects our single pulse search is sensitive to. We used a DM = 500 pc cm^{-3}, a coherent mode gain, and pulse widths from $t_{\rm samp}$ to 0.1 s for the search sensitivity in Fig. 2. It can be seen from Fig. 2 that our search was sensitive to FRBs and FRB-like bursts such as some of those from SGR 1935+2154.

4 DISCUSSION & CONCLUSION

NGC 253 is an intriguing target for extragalactic pulsar exploration due to its stellar composition, current star formation, host SNRs, and associated MGFs seen towards this galaxy. The presence of the optically identified SN 1940E is especially interesting for a young pulsar search, since the lifetime of SNRs is considerably shorter than that of pulsars (e.g. Lyne & Graham-Smith 2012). Thus, a population of young pulsars is expected in this galaxy. Such pulsars are more probable to be detected at vast extragalactic distances, since these objects may emit giant single pulses (Johnston & Romani 2003), the flux density of which is orders of magnitude higher than that of ordinary pulsars. We therefore searched for pulsars, magnetars, and FRBs in NGC 253 with MeerKAT. However, Fig. 2 shows that our single-pulse search was more likely to detect FRBs or equivalent bright-emitting objects (such as SGRs) and that we were not sensitive to the detection of MW-type giant pulses from young pulsars.

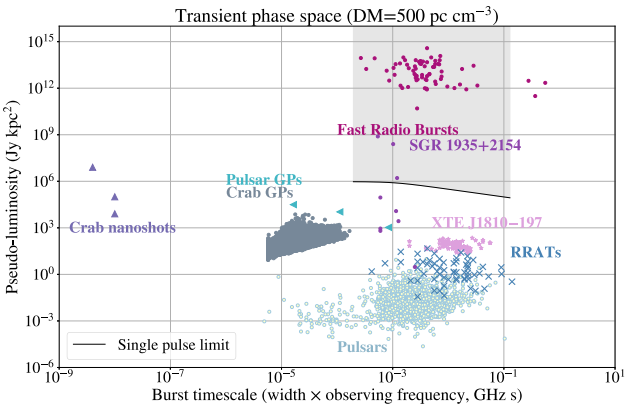

Figure 2. Transient phase space diagram: illustrated in the shaded region is the pseudo-luminosity search limit for our single pulse search. Noticeably, this observation is sensitive to FRBs, including FRB-like bursts of the same pseudo-luminosity as SGR 1935+2154; however, the detection of ordinary pulsars and giant Crab-like pulses is shown to be improbable for our search due to the large distance of NGC 253. Figure and data courtesy of Manisha Caleb.

Surveys such as *The Parkes Southern Pulsar Survey* (Manchester et al. 1996) and *The High Time Resolution Universe Pulsar Survey* (HTRU; Keith et al. 2010) included pointings towards NGC 253, the integration time of which were 157.3 and 270 s, respectively. We searched the entire NGC 253 galaxy, which increased our chances of finding a pulsar as compared to searching only portions of this galaxy. Our integration time is about 52 times longer than that of *HTRU* and our gain is also a factor of 3 times more. Thus, our search with MeerKAT was significantly more sensitive than previous surveys with the Parkes Telescope.

Our periodicity search towards NGC 253 returned no significant candidates. We derived a flux density limit for periodic pulsar signals of $S_{\rm lim,1400MHz} = 4.4$ μJy, which corresponds to a pseudo-luminosity limit of $L_{\rm lim,1400MHz} = 54$ Jy kpc^2. In Fig. 3, we show the cumulative probability distribution of the known MW pulsars from the ATNF catalogue as a function of pseudo-luminosity, with our sensitivity limit indicated by a purple vertical line. The brightest MW pulsar pseudo-luminosity at 1400 MHz from the ATNF catalogue is about 6 Jy kpc^2 (J1644−4559), which is one order of magnitude lower than this limit. Since the pulsar population in the MW spans about six orders of magnitude in pseudo-luminosity, and the maximum pseudo-luminosity is not known, we may be able to probe the upper range of this function. If this luminosity function is taken to be somewhat universal (since NGC 253 is experiencing a period of rapid star formation and has a mass difference of about 50 per cent

[11] http://github.com/jeffzhen/gsm2016

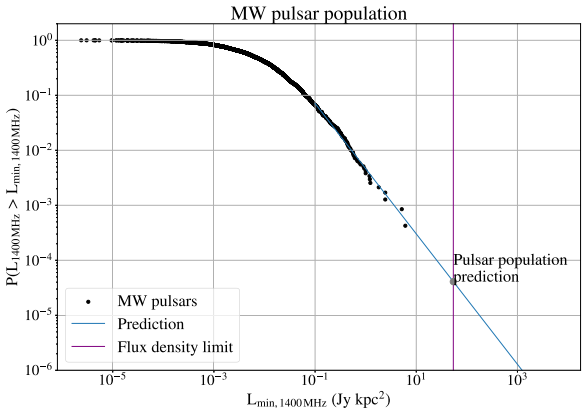

Figure 3. Pseudo-luminosity distribution of the MW pulsar population compared to our survey search limits. Figure produced with ATNF catalogue version 2.0.0.

compared to the MW), it is therefore not unreasonable to search for pulsars in NGC 253. Fitting a power law above $\sim$0.1 Jy kpc^2 ($\sim$0.25, $\sim$0.6 Jy kpc^2) and extrapolating, given the shape of the tail of the distribution at this point, we estimate that the chance of finding a pulsar as bright as our limit is approximately 4.10×10^{-5} (2.51×10^{-5}, 4.25×10^{-5}). Thus, in order to detect such a pulsar in NGC 253, this galaxy should have a pulsar population of at least 2.4×10^4 (3.9×10^4, 2.3×10^4). This is not an unreasonable number, and is a good fraction of the estimated total population of detectable MW pulsars of 122 000 (including millisecond and normal pulsars; Swiggum et al. 2014). This implies that approximately 5 MW pulsars as bright as our limit should exist (slightly more if one integrates up to a certain maximum pseudo-luminosity to include all those exceeding the current (vertical line in Fig. 3) sensitivity limit). However, no such pulsars have been detected to date. This might be due to unfavourable beaming, excessive DM smearing, or obstruction by other sources. Alternatively, the luminosity distribution might cut off earlier (departing from the power-law tail), implying a strict upper limit on the maximum pseudo-luminosity of $L_{\rm cut,1400MHz} \lesssim L_{\rm lim,1400MHz}$ for both galaxies, and in this case, we should not expect to see such a bright pulsar in NGC 253. Otherwise, the luminosity distributions may be different between the galaxies, reflecting distinct star-formation histories. MW pulsars have typical conversion efficiencies (η) of radio emission derived from the pulsar rotational spin-down luminosity $\dot{E}_{\rm rot}$ of 10^{-8}–10^{-5} (e.g. Szary et al. 2014). Given our periodic-signal sensitivity limit, a Crab-like pulsar with $\dot{E}_{\rm rot} \sim 5 \times 10^{38}$ erg s^{-1} should have been detectable if $\eta \gtrsim 10^{-8}$. Conversely, for a typical value of $\eta \sim 10^{-5}$, a pulsar with $\dot{E}_{\rm rot} \sim 5 \times 10^{35}$ erg s^{-1} should have been detectable.

Moving to single-pulse searches, as seen in Fig. 2, we were sensitive to FRB and FRB-like pulse detections. We derived a single-pulse flux density limit of approximately 62 mJy for our FRB search in the direction of NGC 253. This limit is orders of magnitude lower than the flux density of previously detected FRBs. Since two MGFs are associated with NGC 253 (Svinkin et al. 2021; Trigg et al. 2024), we would expect to be able to observe bursts similar to those of SGR J1935+2154 in the MW, should they have occurred. However, our non-detection can potentially be due to the epoch of observation, since these events are unpredictable and sporadic. It can also be due to unfavourable orientations. Transient radio emission, lasting for years have also been seen from magnetars, but none has been associated with MGFs, since these events are rare and not much radio follow-up has been possible (Camilo et al. 2006; Levin et al. 2019).

Future observations covering a longer integration time may uncover pulsars and FRBs in this and other nearby galaxies.

ACKNOWLEDGEMENTS

We thank the anonymous referee for their constructive feedback that helped improve the quality of the paper. The MeerKAT telescope is operated by the South African Radio Astronomy Observatory, which is a facility of the National Research Foundation (NRF), an agency of the Department of Science and Innovation (DSI). SARAO acknowledges the ongoing advice and calibration of GPS systems by the National Metrology Institute of South Africa (NMISA) and the time space reference systems department of the Paris Observatory. TRAPUM observations used the FBFUSE and APSUSE computing clusters for data acquisition, storage and analysis. These clusters were designed, funded and installed by the MAX-PLANCK-INSTITUT für Radioastronomie and the Max-Planck Gesellschaft. This work is based on research supported in part by the NRF. CV acknowledges that opinions, findings, and conclusions or recommendations expressed in any publication generated by the NRF-supported research are those of the author(s), and that the NRF accepts no liability whatsoever in this regard. HH acknowledges research support in part by the NRF of South Africa (Grant number 142859), and support through the National Astrophysics and Space Science Program (NASSP), funded by NRF. RPB acknowledges support from the European Research Council (ERC) under the European Union's Horizon 2020 research and innovation program (grant agreement No. 715051; Spiders) This research has made use of hips2fits,[12] a service provided by CDS, the SIMBAD data base, operated at CDS, Strasbourg, France (Wenger et al. 2000), NASA's Astrophysics Data System Bibliographic Services, and the ATNF pulsar catalogue version 2.0.0. and 2.3.0. Fig. 1 was made using the APLpy version 2.1.0 (Robitaille & Bressert 2012; Robitaille 2019), which is an open-source astronomy plotting PYTHON package.

DATA AVAILABILITY

The data underlying this article will be shared upon reasonable request to the TRAPUM collaboration.

REFERENCES

Badenes C., Maoz D., Draine B. T., 2010, MNRAS, 407, 1301
Bailes M. et al., 2020, Publ. Astron. Soc. Aust., 37, e028
Barnes A. T., Longmore S. N., Battersby C., Bally J., Kruijssen J. M. D., Henshaw J. D., Walker D. L., 2017, MNRAS, 469, 2263
Barr E. D., 2017, Proc. IAU, 13, 175
Barr E., 2020, Peasoup: C++/CUDA GPU pulsar searching library, Astrophysics Source Code Library, record (ascl:2001.014)
Barsdell B. R., Bailes M., Barnes D. G., Fluke C. J., 2012, MNRAS, 422, 379
Bhandari S. et al., 2022, AJ, 163, 69
Bochenek C. D., Ravi V., Belov K. V., Hallinan G., Kocz J., Kulkarni S. R., McKenna D. L., 2020, Nature, 587, 59
Bochenek C. D., Ravi V., Dong D., 2021, ApJ, 907, L31
Camilo F., 2018, Nat. Astron., 2, 594

[12] https://alasky.cds.unistra.fr/hips-image-services/hips2fits

Camilo F., Ransom S. M., Halpern J. P., Reynolds J., Helfand D. J., Zimmerman N., Sarkissian J., 2006, Nature, 442, 892
Camperi J. A., Dottori H., Günthardt G., Díaz R. J., Vega Neme L. R., Agüero M. P., 2022, BAAA, 63, 232
Carli E. et al., 2024, MNRAS, 531, 2835
Chen W., Barr E., Karuppusamy R., Kramer M., Stappers B., 2021, J. Astron. Instrum., 10, 2150013
Chhetri R., Morgan J., Ekers R. D., Macquart J. P., Sadler E. M., Giroletti M., Callingham J. R., Tingay S. J., 2018, MNRAS, 474, 4937
CHIME/FRB Collaboration et al., 2020, Nature, 587, 54
CHIME/FRB Collaboration et al., 2021, ApJS, 257, 59
Cordes J. M., Lazio T. J. W., 2003, NE2001.I. A New Model for the Galactic Distribution of Free Electrons and its Fluctuations, preprint (arXiv:astro-ph/0207156)
Crawford F., Kaspi V. M., Manchester R. N., Lyne A. G., Camilo F., D'Amico N., 2001, ApJ, 553, 367
Davidge T. J., 2016, ApJ, 818, 142
Dewey R. J., Taylor J. H., Weisberg J. M., Stokes G. H., 1985, ApJ, 294, L25
Duarte Puertas S., Vilchez J. M., Iglesias-Páramo J., Mollá M., Pérez-Montero E., Kehrig C., Pilyugin L. S., Zinchenko I. A., 2022, A&A, 666, A186
Forbes D. A., Ward M. J., Rotaciuc V., Blietz M., Genzel R., Drapatz S., van der Werf P. P., Krabbe A., 1993, ApJL, 406, L11
Gaensler B. M., 2004, Adv. Space Res., 33, 645
Geyer M. et al., 2021, MNRAS, 505, 4468
Heger A., Fryer C. L., Woosley S. E., Langer N., Hartmann D. H., 2003, ApJ, 591, 288
Heintz K. E. et al., 2020, ApJ, 903, 152
Hisano S. et al., 2022, ApJ, 928, 161
Jankowski F., van Straten W., Keane E. F., Bailes M., Barr E. D., Johnston S., Kerr M., 2018, MNRAS, 473, 4436
Johnston S., Romani R. W., 2003, ApJ, 590, L95
Jonas J., MeerKAT Team, 2016, Proc. Sci., The MeerKAT Radio Telescope. SISSA, Trieste, PoS(MeerKAT2016)001
Karachentsev I. D., Tully R. B., Anand G. S., Rizzi L., Shaya E. J., 2021, AJ, 161, 205
Keith M. J. et al., 2010, MNRAS, 409, 619
Koehn H. et al., 2024, preprint (arXiv:2402.04172)
Kornei K. A., McCrady N., 2009, ApJ, 697, 1180
Kouwenhoven M. L. A., Voûte J. L. L., 2001, A&A, 378, 700
Levin L. et al., 2019, MNRAS, 488, 5251
Levin L., 2012, PhD thesis, Swinburne University of Technology, Australia
Longmore S. N. et al., 2013, MNRAS, 429, 987
Lorimer D. R., Bailes M., McLaughlin M. A., Narkevic D. J., Crawford F., 2007, Science, 318, 777
Lundgren S. C., Cordes J. M., Ulmer M., Matz S. M., Lomatch S., Foster R. S., Hankins T., 1995, ApJ, 453, 433
Lyne A., Graham-Smith F., 2012, Pulsar astronomy. No. 48, Cambridge University Press, Cambridge, UK
Manchester R. N. et al., 1996, MNRAS, 279, 1235
Manchester R. N., Fan G., Lyne A. G., Kaspi V. M., Crawford F., 2006, ApJ, 649, 235
Manchester R. N., Hobbs G. B., Teoh A., Hobbs M., 2005, AJ, 129, 1993
Mannings A. G. et al., 2021, ApJ, 917, 75
Marnoch L. et al., 2020, A&A, 639, A119
McLaughlin M. A., Cordes J. M., 2003, ApJ, 596, 982
Men Y., Barr E., 2024, A&A, 683, A183
Men Y., Barr E., Clark C. J., Carli E., Desvignes G., 2023, A&A, 679, A20
Mills E. A. C. et al., 2021, ApJ, 919, 105
Morello V., Barr E. D., Stappers B. W., Keane E. F., Lyne A. G., 2020, MNRAS, 497, 4654
Morello V. et al., 2018, MNRAS, 483, 3673
Padmanabh P. V. et al., 2023, MNRAS, 524, 1291
Philippov A., Kramer M., 2022, ARA&A, 60, 495
Platts E., Weltman A., Walters A., Tendulkar S. P., Gordin J. E. B., Kandhai S., 2019, Phys. Rep., 821, 1
Ransom S., 2011, PRESTO: PulsaR Exploration and Search TOolkit. Astrophysics Source Code Library, record (ascl:1107.017)
Rekola R., Richer M., McCall M. L., Valtonen M., Kotilainen J., Flynn C., 2005, MNRAS, 361, 330
Robitaille T., 2019, APLpy v2.0: The Astronomical Plotting Library in Python (2.0). Zenodo. Available at: https://doi.org/10.5281/zenodo.2567476
Robitaille T., Bressert E., 2012, APLpy: Astronomical Plotting Library in Python. Astrophysics Source Code Library, record (ascl:1208.017)
Spitler L. G. et al., 2016, Nature, 531, 202
Stappers B., Kramer M., 2016, Proc. Sci., An Update on TRAPUM. SISSA, Trieste, PoS(MeerKAT2016)009
Svinkin D. et al., 2021, Nature, 589, 211
Swiggum J. K. et al., 2014, ApJ, 787, 137
Szary A., Zhang B., Melikidze G. I., Gil J., Xu R.-X., 2014, ApJ, 784, 59
Taylor J. H., Fowler L. A., McCulloch P. M., 1979, Nature, 277, 437
Thornton D. et al., 2013, Science, 341, 53
Titus N., Stappers B. W., Morello V., Caleb M., Filipovic M. D., McBride V. A., Ho W. C. G., BuckleyD. A. H., 2019, MNRAS, 487, 4332
Titus N., Toonen S., McBride V. A., Stappers B. W., Buckley D. A. H., Levin L., 2020, MNRAS, 494, 500
Trigg A. C. et al., 2024, A&A, 687, A173
Wenger M. et al., 2000, A&AS, 143, 9
Wik D. R. et al., 2014, ApJ, 797, 79
Yao J. M., Manchester R. N., Wang N., 2017, ApJ, 835, 29
Zheng H. et al., 2017, MNRAS, 464, 3486
Zhu W. W. et al., 2014, ApJ, 781, 117
Zwicky F., 1941, IAU Circulars, 848

This paper has been typeset from a TEX/LATEX file prepared by the author.